

Enhancing PCB Motor Performance through Phase Resistance Reduction in Slotted PCB Motors with Ferrite Core

Shahin Asgari^{1,2}, Nejat Saed^{1,2}, Annette Muetze^{1,2}

¹Christian Doppler Laboratory for Brushless Drives for Pump and Fan Applications, Graz, Austria

²Electric Drives and Machines Institute, Graz University of Technology, Graz, Austria

Abstract— In the highly competitive automotive industry, minimizing production costs while maintaining product performance is a critical design objective, particularly for mass-produced devices. A recently introduced cost-effective motor concept tailored to such demands is a three-phase axial flux permanent magnet motor topology that employs a printed circuit board (PCB) instead of a conventional winding with a ferrite core, thereby reducing the drive's complexity, cost, and component count. The main focus of this study is implementing different strategies to minimize the phase resistance of PCB motors. A comparative analysis between the existing PCB design for a PCB motor with a ferrite core and the enhanced version of the PCB with reduced resistance has been done. The validation of simulation outcomes has been reinforced through precise experimental measurements, thereby enhancing the reliability of the conclusions.

Keywords— PCB motor, ferrite core, ferrite magnet, FEA analysis

I. INTRODUCTION

The conventional method of manufacturing electric motor cores involves punching and stacking steel sheets, which is cost-effective for radial flux machines. Using laminated cores in axial flux machines increases complexity and manufacturing costs [1]. The design includes stacking sheets together to form a core perpendicular to the machine's axial direction, creating small air gaps that decrease magnetic flux density and performance. Additionally, core design intricacies make manufacturing and alignment difficult, especially for small drives. This approach poses challenges for axial flux motors and can influence the magnetic characteristics of electrical steels [2], which could be significant in small drives. An alternative option is to manufacture an axial flux permanent magnet (AFPM) core using soft magnetic composite [3]. SMCs offer advantages such as high magnetic flux densities, ease of manufacturing for AFPM cores, and reduced eddy current losses due to high electrical resistivity. However, SMCs are more expensive than steel sheets and are most beneficial when using strong magnets to produce high flux density in the air-gap and high torque densities. Soft ferrite materials are popular choices for core materials in high-frequency transformers and inductors [4], especially in power electronic applications. They offer low eddy current losses even at high frequencies (from kilohertz to megahertz) due to their high electrical resistivity. Ferrite materials have

advantages such as lightweight construction, high magnetic permeability, affordability, and operational efficiency across a wide temperature range. While ferrite has a higher relative cost and lower flux density saturation compared to steel sheets, these factors are not crucial when using inexpensive and weak magnets. The simplicity of ferrite's manufacturing process allows for versatile shaping through ceramic manufacturing techniques. Unlike metals, ferrite can be directly molded, machined, and polished to precise tolerances.

PCB technology presents a compelling alternative to the conventional approach of coil winding for the armature of AFPMs. The application of a multi-layer PCB design has demonstrated its efficacy in the fabrication of small motors. The primary benefits inherent in the integration of PCB stators within AFPMs encompass streamlined manufacturing and maintenance processes, alongside the attainment of minimized torque output fluctuations.

A comprehensive framework is outlined in [5], aiming to conceive and assess AFPMs that are lightweight, cost-efficient, and incorporate dual permanent magnet rotors along with a coreless PCB stator. Furthermore, the [6,7] delve into an in-depth exploration of the computation of eddy currents and associated losses within PCB circuits. Addressing the concept discussed in [8], the feasibility of employing slotted and slot-less AFPMs featuring PCB winding is proposed. Notably, it has been ascertained that the torque density of slotted machines notably surpasses that of slot-less machines, although the intricate geometrical design of the former may give rise to manufacturing complexities.

A noteworthy drawback encountered in compact slotted PCB motors is the low filling factor and high stator resistance they exhibit, which can limit the current injection through the stator winding, especially in low-voltage applications, and impede motor initiation under diverse circumstances. In response, this research introduces criteria and strategies for reducing the stator resistance of an axial flux PCB motor with a ferrite core (PCBFC) to enhance the motor's performance while the source voltage is constant.

II. THE PCB MOTOR STRUCTURE

The proposed PCB motor topology features a ferrite stator core, PCB winding, and ferrite magnets which have been depicted in Fig. 1. The stator core material must function at higher frequencies, be cost-effective for small AFPMs, and does not require a high saturation point due to ferrite PMs' low residual flux density. Based on these requisites, ferrite has

The financial support by the Austrian Federal Ministry for Digital and Economic Affairs and the National Foundation for Research, Technology, and Development is gratefully acknowledged.

been chosen as the primary material for the proposed PCB motor core, featuring 24 slots and a circular cross-section for ease of assembly and cost savings in PCB production. The prototype utilizes 3C90 ferrite, suitable for frequencies up to 0.2 MHz with a saturation point of 0.47 T, estimating a motor working frequency of 1000 Hz to 1500 Hz depending on the rotational speed.

The stator winding on the PCB employs copper traces in a three-phase motor with a delta configuration, consisting of eight coils per phase. Integrating control and supply circuits onto the same PCB as the stator reduces the motor's overall size and cost.

In contrast to coreless PCB motors requiring costly Neodymium Iron Boron (NdFeB) magnets, the PCBFC motor utilizes ferrite permanent magnets with a residual flux density of 0.275 T. To cut production costs, the rotor omits back-iron and uses separate magnet segments glued to a plastic frame for prototyping. The rotor comprises a non-ferromagnetic rotor yoke and a 28-pole permanent magnet.

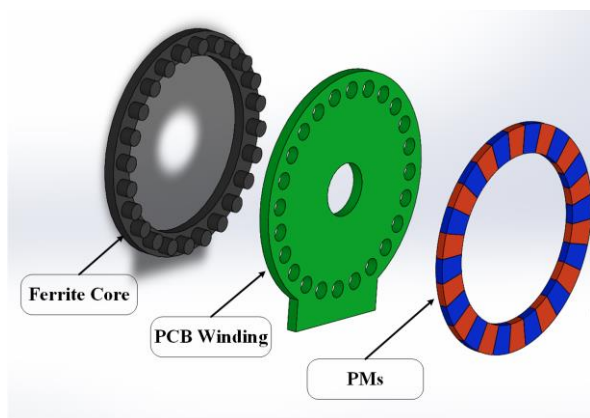


Fig. 1. The PCB motor structure.

III. STRATEGIES FOR RESISTANCE REDUCTION

The primary distinction between PCB motors and conventional motors concerns their windings. PCBs primarily function in the transmission of signals between electronic and power components, which renders them unsuited for carrying substantial currents, as conventional electric drive windings do. Even when dealing with small-sized electric motors, the required current is notably higher than that typically encountered within electronic boards. While there might be certain specialized compact drives that could utilize PCB windings within their feasible current range, it's essential to note that the resistance of such windings surpasses that of conventional windings.

This challenge becomes more pronounced in cases where the voltage source needs to be restricted to a lower magnitude, as is often the scenario in automotive applications. The injection of current into the motor windings becomes difficult due to the elevated resistivity inherent in these conditions. In the next subsections, the criteria of PCB winding and the methods to reduce resistance being introduced.

A. Turn Numbers and Winding Layout

Three fundamental principles crucial to the design of PCB windings encompass the minimum track width, the minimum clearance amid the track and the edge, and the thickness of the copper layer. It is evident that a more substantial copper layer

holds the potential to curtail resistance, albeit at the expense of escalated costs and an increased minimum clearance requirement. Conversely, the utmost track width finds limitations aligned with the highest operational frequency. The clearance emerges as the predominant factor dictating the filling factor of the PCB winding. This aspect becomes especially pronounced in slotted PCB motors, wherein a substantial portion of the PCB surface remains unutilized due to its occupation by stator teeth. In comparison with core-less PCB motors, this type exhibits a comparatively diminished usable surface.

The PCB manufacturer establishes the minimum clearance, with the standard dimensions being a hundred microns between two tracks and two hundred microns between a track and the edge. Although this minimum clearance remains fixed, altering the number of turns in the winding results in a corresponding variation in the number of clearances. Consequently, an increase in the number of turns leads to a reduction in the filling factor, elevating the total resistance. This underscores the importance of meticulous calculation of the winding's turn number during the initial stages of PCB winding design, in contrast to the conventional round copper winding approach.

In the case of conventional winding utilizing enameled wire, the coating thickness spans between 1 and 20 μm , contingent on the spectral width. In low-voltage applications, this thickness approximates three micro meter. For comparison, this dimension amounts to 100 μm between two tracks.

Based on the elucidation provided in the preceding section, it has been concluded that reducing the number of turns per coil while the back-EMF stays constant results in reducing the total resistance. In pursuit of this objective, a new winding layout has been implemented, boasting a higher winding factor than its predecessor. The layouts are presented in Fig. 2. Notably, a transformation from a delta connection to a star connection has been applied to the end winding. These dual enhancements have collectively facilitated a reduction in the number of turns from nine to five.

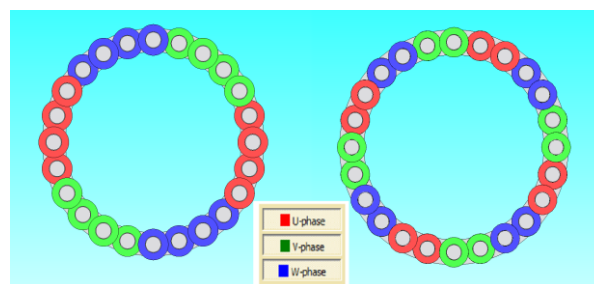


Fig. 2. PCB motor layouts; left side: first design and right side: new design.

The outcomes of simulations for both designs, conducted at 5000 revolutions per minute, are portrayed in Fig. 3. It is worth highlighting that, despite the lower turn count in comparison to the initial design, the back-EMF remains unchanged. Intriguingly, the new design exhibits a marginally elevated back-EMF when juxtaposed with the first design.

Fig. 4 provides an illustrative cross-sectional view of a layer of PCB situated between two teeth. The copper layer boasts a thickness of 35 μm . In the layout of a five-turn configuration with a width occupied by copper amounting to 284 μm , the resultant filled width measures 1420 μm .

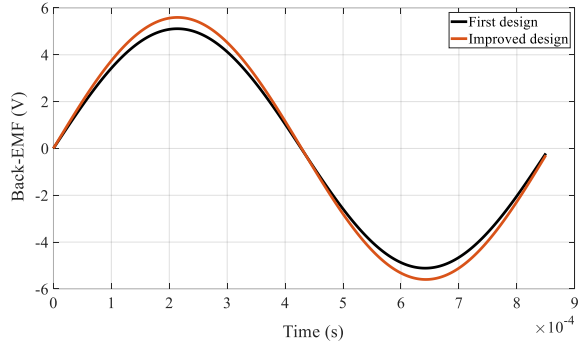


Fig. 3. Back-EMF waveform; @5000 rpm the software JMAG® [9] is used.

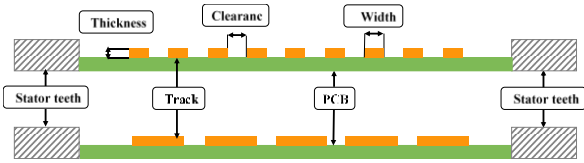


Fig. 4. Cross-sectional view of PCB; Top: first PCB design and bottom: improved PCB design.

Conversely, for a nine-turn configuration with a 100 μm width, the filled width spans 900 μm , signifying a noteworthy increase of 57 percent. Furthermore, the coil's length has undergone a reduction of 55 percent owing to the decrease in the number of turns per coil. These dual enhancements have substantially mitigated the total resistance per coil.

B. Impact of Track Width on Conductor Cross-Section

In theoretical terms, the cross-section of a track is rectangular. However, in practical manufacturing processes undertaken by PCB manufacturers, this rectangular configuration undergoes alteration. As depicted in Fig. 5(a), a genuine cross-section of a PCB reveals a trapezoidal shape, with the track width corresponding to the base of this trapezoid. This transformation from a rectangle to a trapezoid invariably leads to a reduction in the actual conductor area in comparison to the anticipated rectangular area, as depicted in Fig. 5(b). Consequently, any augmentation in the area does not exhibit a linear correlation with the increment in track width. This is particularly significant as resistance is contingent upon the cross-sectional area of the conductor.

The relationship between the area of the trapezoid and the area of the rectangle is contingent upon the width and the corner angle. This ratio can be determined by calculating the area illustrated in Fig. 5(b) as:

$$\frac{S_{\text{Trapezoid}}}{S_{\text{Rectangle}}} = \frac{W - h \cot \alpha}{W} \quad (1)$$

Where W is the track, h is copper thickness and α is the base angle.

The base angle of the trapezoid can indeed vary based on factors such as copper thickness and the specifics of the manufacturing process. Empirical measurements taken from prototyped PCBs indicate that, for a copper thickness of 35 μm , the approximate value of this angle is around 56

degrees. This observed variation underscores the influence of material properties and fabrication techniques on the resulting geometry.

The alteration in the effective surface area of the conductor has been visually represented for three distinct base angles as determined by (1), in Fig. 5. Over a range where the width has been expanded from 100 μm (representing the minimum width) to 1 mm, a discernible pattern emerges. It becomes evident that an escalation in track width results in a non-linear augmentation in the effective area. Consequently, the selection of the minimum track width is less optimal. Conversely, by enhancing the design and increasing the track width to 284 μm , the effective surface area is bolstered by approximately 15 percent. This enhancement in effective surface area, in turn, contributes to a reduction in the overall coil resistance, underlining the benefits of this approach.

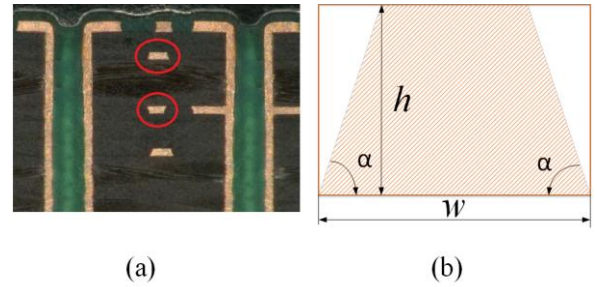


Fig. 5. PCB tracks; (a) cross-section of a track[10], (b) effective surface.

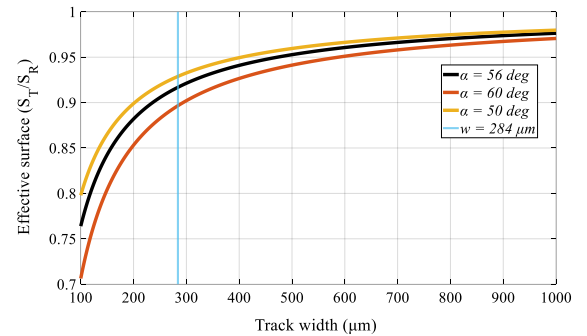


Fig. 6. Variation of effective surface with changes in track width

C. Modification of Track's Radial Width

The primary constraint when arranging tracks for a PCB motor with a ferrite core lies in the spacing between two teeth, similar to the slot area in a conventional winding structure. Fig. 7 shows the initial design for the PCB winding, where the track width remains uniform in all orientations and matches the maximum distance between two teeth. An appealing opportunity presents itself within the common core dimensions and PCB layout, involving the use of unoccupied PCB space to enhance track width in the radial direction. This potential arises from available space both inside and outside of the teeth area. Enlarging the track width in this manner contributes to a reduction in coil resistance and subsequently, the overall resistance of each phase.

The enhanced design, detailed in Fig. 8, incorporates five turns per coil and wider tracks in the radial direction. For a comprehensive comparison, the specifications of both the initial design and the improved design are tabulated in Table I.

TABLE I. PCB SPECIFICATIONS

Parameter	1 st	2 nd	Parameter	1 st	2 nd
PCB layer	8	8	Phase resistance	45 Ω	5.8 Ω
Phase turns	288	160	Min track width	0.1 m m	0.28 mm
Coil no.	8	8	Min clearance	0.1 m m	0.1 mm
Coil Turns	9	5	PCB diameter	50 mm	56 mm

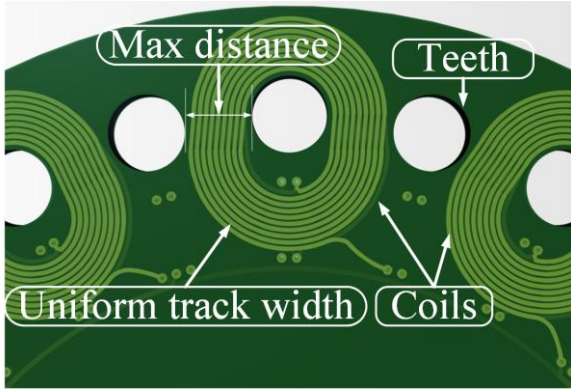


Fig. 7. First design PCB.

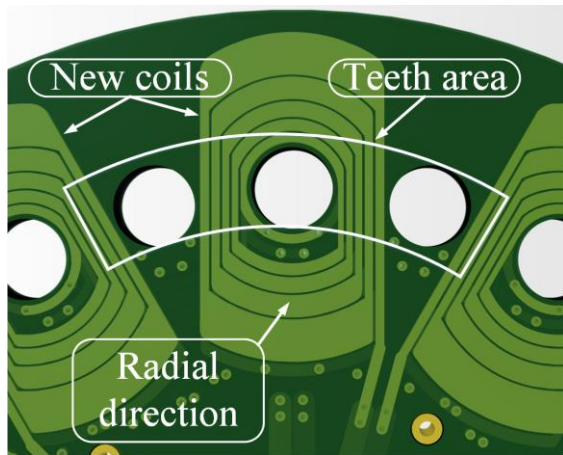


Fig. 8. Improved design PCB.

IV. PERFORMANCE ANALYSIS

The resistance measurements conducted on the prototype PCBs reveal a substantial reduction in the resistance of each phase, dropping from 45 ohms to 5.8 ohms in the enhanced design. This transformation marks a significant advancement in resistance reduction. Furthermore, the outer diameter of the PCB has expanded from 50 mm to 55 mm, reflecting a 10 percent increase.

In order to examine the influence of resistance reduction on motor performance, two separate 3D Finite Element Analysis (FEA) studies were conducted. These analyses maintained consistent parameters, with the sole distinction being the variations in the designs of the PCBs. The simulation results reveal that under a constant source voltage of 12 volts, the generated output torque escalated from 2 mN·m to 5.5 mN·m. This boost in torque is attributable to the feasibility of injecting a more substantial current into the motor while

maintaining the same voltage. Furthermore, the efficiency underwent enhancement from 38 percent to 48 percent. While efficiency might not be the predominant focal point in the design of small machines, its improvement contributes to the motor's capacity to operate under cooler conditions while sustaining the same output power.

Fig. 9 and 10 present a comprehensive comparison of the line voltage and phase current for both initial design and the enhanced version. Evidently, the input voltage remains proximate to 12 volts, yet the consumption current surpasses that of the initial design. It's imperative to acknowledge that the phase current is scaled by a factor of 4.16, accompanied by a 3.4-fold augmentation in the average cross-sectional area of the conductor. Consequently, the current density in the improved design has observed an 18 percent increase, which still maintains its status within an acceptable range.

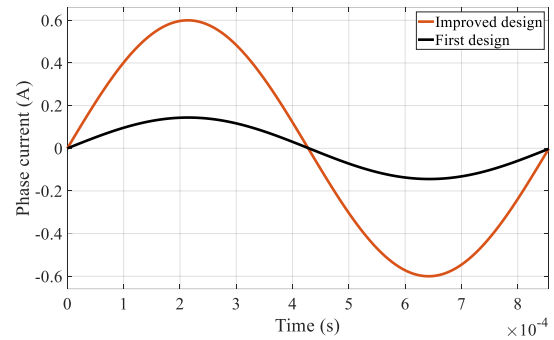


Fig. 9. Phase current waveform.

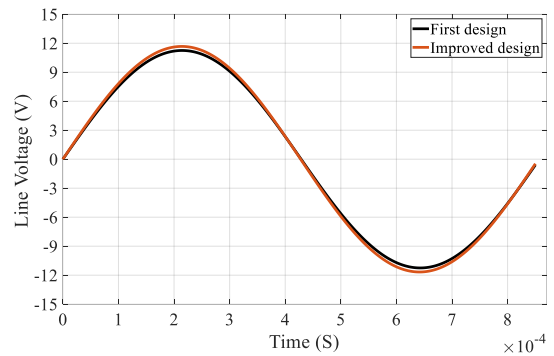


Fig. 10. Line to line input voltage.

V. CONCLUSION

This investigation is dedicated to the meticulous redesign of the copper trace width within a printed circuit board (PCB), with the overarching aim of diminishing the resistance inherent in the winding of a slotted PCB motor featuring a ferrite core. Notably, this enhancement process has yielded a discernible augmentation in the average output torque of the motor, rendering it better suited for 12-volt applications. To verify the efficacy of the optimized PCB, precise prototyping and resistance measurements of PCBs were carried out. The validation of motor performance enhancement was further substantiated through the utilization of finite-element analysis.

Furthermore, a comparative analysis was conducted to assess the operational efficiency of the motor equipped with the improved PCB design in contrast to the initial design. This comparison encompassed the simulation of back-EMF and

output torque, effectively illustrating the tangible benefits conferred by the improvement process.

ACKNOWLEDGMENT

The authors are grateful to MSG Mechatronic Systems GmbH, Wies, Austria, Dr.techn. Klaus Krischan, and Dipl.-Ing. Benedikt Riegler for their valuable contribution.

REFERENCES

- [1] Gieras J.: Wang R. J.: Kamper M. J.: Axial Flux Permanent Magnet Brushless Machines, Springer Science, Inc. Kluwer Academic Publishers, 2005.
- [2] M. Bali and A. Muetze, "Influence of Different Cutting Techniques on the Magnetic Characteristics of Electrical Steels Determined by a Permeameter," in IEEE Transactions on Industry Applications, vol. 53, no. 2, pp. 971-981, March-April 2017, doi: 10.1109/TIA.2016.2617305.
- [3] R. Tsunata, M. Takemoto, S. Ogasawara, T. Saito and T. Ueno, "SMC Development Guidelines for Axial Flux PM Machines Employing Coreless Rotor Structure for Enhancing Efficiency Based on Experimental Results," in IEEE Transactions on Industry Applications, vol. 58, no. 3, pp. 3470-3485, May-June 2022, doi: 10.1109/TIA.2022.3154336.
- [4] G. Zhu and D. Gao, "Improving Quality Factor of Ferrite-Core Inductors Applied in Inductive Power Transfer," 2021 IEEE 4th International Electrical and Energy Conference (CIEEC), Wuhan, China, 2021, pp. 1-6, doi: 10.1109/CIEEC50170.2021.9510543.
- [5] B. Anvari, P. Guedes-Pinto and R. Lee, "Dual Rotor Axial Flux Permanent Magnet Motor using PCB Stator," 2021 IEEE International Electric Machines & Drives Conference (IEMDC), Hartford, CT, USA, 2021, pp. 1-7, doi: 10.1109/IEMDC47953.2021.9449506
- [6] A. Bauer, C. Schumann and S. Urschel, "Analytical Calculation of Eddy Current related Losses and Parasitic Torque in PCB Windings," 2022 International Conference on Electrical Machines (ICEM), Valencia, Spain, 2022, pp. 1750-1756, doi: 10.1109/ICEM51905.2022.9910682.
- [7] X. Wang, T. Li, P. Gao and X. Zhao, "Design and Loss Analysis of Axial Flux Permanent Magnet Synchronous Motor with PCB Distributed Winding," 2021 24th International Conference on Electrical Machines and Systems (ICEMS), Gyeongju, Korea, Republic of, 2021, pp. 1112-1117, doi: 10.23919/ICEMS52562.2021.9634627.
- [8] Karabulut Y.: Meşe E.: Torque Performance Comparison Between Slotted and Non-Slotted Axial Flux PCB Winding Machine, 2021 IEEE 19th International Power Electronics and Motion Control Conference (PEMC), pp. 519-523. 2021.
- [9] JSOL Corporation: Simulation Technology for Electro-Mechanical Design, <http://www.jmag-international.com>, accessed on 31-05-2023.
- [10] Multi-Circuit-Boards: Printed Circuit Boards Manufacturing, <https://www.itwm.fraunhofer.de>, accessed on 31-06-2023.